ELSEVIER

Thermochimica Acta 367–368 (2001) 217–227

thermochimica acta

www.elsevier.com/locate/tca

Heat capacity measurement by sawtooth modulated standard heat-flux differential scanning calorimetry with sample temperature control☆

M. Pyda[a,b], Y.K. Kwon[a,b], B. Wunderlich[a,b,*]

[a]*Department of Chemistry, University of Tennessee, Knoxville, TN 37996-1600, USA*
[b]*Chemical and Analytical Sciences Division, Oak Ridge National Laboratory, Oak Ridge, TN 37831-6197, USA*

Received 1 October 1999; accepted 28 April 2000

Abstract

The frequency dependence of the apparent heat capacity is analyzed when measuring with a heat-flux type, standard differential scanning calorimetry (DSC), controlled at the sample. A specially constructed, centrosymmetric sawtooth modulation composed of 14 heating and cooling segments was used for the measurements. This complex sawtooth produces four harmonics of the order $v = 1, 3, 5$ and 7 with close to equal amplitudes in the Fourier representation. A single measurement should thus be sufficient for the evaluation of the frequency dependence of the measured, apparent heat capacity from the amplitudes of the Fourier series of the differential heat-flow rate (A_{HF}) and the sample temperature (A_{T_s}). The frequency independent heat capacity can, however, not be represented by the expression: $C_p = A_{HF}/(A_{T_s} v\omega)[1 + (\tau v\omega)^2]^{0.5}$, with a fixed τ, as is possible with a sinusoidal modulation which keeps the DSC in steady state, but τ depends on sample and reference properties, as well instrument parameters such as pan masses and thermal contacts, and may also be influenced by the design of the control and analysis software. Published by Elsevier Science B.V.

Keywords: Heat capacity; Temperature-modulated differential scanning calorimetry; TMDSC; Fourier transformation; Higher harmonics; Sawtooth modulation

1. Introduction

Heat capacity can be determined with three techniques, adiabatic calorimetry, standard differential scanning calorimetry (DSC), and temperature-modulated differential scanning calorimetry (TMDSC). In adiabatic calorimetry, heat capacity is usually determined at low temperature (0–300 K) by direct measurement of heat input and the corresponding temperature change of the sample [1]:

$$C_p = \frac{\Delta Q(\text{corrected})}{\Delta T(\text{corrected})}. \quad (1)$$

Elaborate instrumentation and loss calculations are needed to correct for the deviation from fully adiabatic conditions, but a precision from 0.1 to 1% is often reached.

* Corresponding author. Present address: Department of Chemistry, University of Tennessee, Knoxville, TN 37996-1600, USA.
E-mail address: athas@utk.edu (B. Wunderlich).

0040-6031/01/$ – see front matter Published by Elsevier Science B.V.
PII: S0040-6031(00)00697-3

In a standard DSC experiment, much of the loss and gain of heat is compensated by the differential mode of operation. Furthermore, many of the kinetic aspects resulting from the scanning operation are eliminated by considering only data generated after steady state is reached. The effect of the remaining difference in heating rate between reference and sample calorimeter is small, and can easily be corrected for, without the need of any additional calibration [1].

At steady state, all points in the twin calorimeters are expected to increase with the same heating rate q. The programmed temperature is a linear ramp over a rather large temperature interval (typically 50–100 K) with a heating rate of 5–40 K min^{-1}, and measurements can be made from temperatures between 100 and 1000 K [1]. The difference in temperatures between reference and sample $(T_r - T_s = \Delta T)$ is directly proportional to the heat-flow rate, so that

$$C_p = \frac{\Delta T}{q} K, \tag{2}$$

where the K is obtained by calibration with a calorimetric standard, such as sapphire (Al_2O_3). A typical precision of up to 3% is possible.

In TMDSC, the programmed temperature is produced by superposition of a constant heating rate and a temperature modulation [2,3]. The constant, underlying heating rate corresponds to the average over one modulation period, written as $\langle q \rangle$. The initial modulations provided for TMDSC were sinusoidal (TA Instruments, MDSC 2910^{TM}) and measurements were carried out under conditions which remained close to steady state, even during the modulation. Many measurements were made in the quasi-isothermal mode, i.e., without an underlying heating rate $\langle q \rangle = 0$ [4].

In the quasi-isothermal method of TMDSC, a reversing heat capacity can be evaluated from the amplitudes of the heat-flow rate AHF and the corresponding sample temperature, A_{T_s} [5]:

$$C_p = \frac{A_{HF}}{A_{T_s}\omega} K(\omega), \tag{3}$$

where ω is the frequency in rad s^{-1} ($=2\pi/p$, with p representing the modulation period in s) and $K(\omega)$ corrects for the different modulation in the reference calorimeter ($= [1 + (C_r\omega/K)^2]^{0.5}$, with C_r representing the heat capacity of the reference calorimeter and K, the Newton's law constant as also given for the DSC, Eq. (2)). Note that $A_{T_s}\omega$ is the amplitude of the heating rate dT/dt. The amplitudes are extracted from the raw data, gathered as a function of time, by the first harmonic of the Fourier transform from the time- to the frequency-domain. All extraneous heat losses which are different in frequency from ω are thus eliminated, improving the quality of the measurement. Ultimately, it is expected that the precision of TMDSC will reach that of adiabatic calorimetry.

The same analysis method can also be used with an underlying heating rate $\langle q \rangle$ by subtracting the averages of the heat-flow (proportional to ΔT) and heating rates in a pseudo-isothermal analysis [5]. This is equivalent to subtracting the constant contributions in the Fourier transformation. The sliding averaging over one modulation period yields the total heat-flow rate, which is proportional to ΔT in Eq. (2) and contains all heat effects (including most losses). The amplitude of the reversing heat-flow rate A_{HF} in Eq. (3), in contrast, contains only contributions from the first harmonic of the Fourier series. For calorimetry without losses and outside of transition regions, both, the total and the reversing heat capacities in Eqs. (2) and (3) should be identical. Within transition regions (and whenever heat losses or deviations from ideal measurement conditions occur) a nonreversing heat capacity is observed as the difference between total and reversing heat capacities.

When using a sawtooth for modulation, complications occur in the data evaluation because steady state is lost on any abrupt change in heating rate, i.e., the simple Eq. (3) does not hold until the time to recover steady state becomes negligible. This time interval may be 100–250 s, depending on the calorimeter construction, and is several times the shortest modulation period p possible for sinusoidal oscillations. In this paper it will be shown how these difficulties can be alleviated for a heat-flux TMDSC of the type with modulation controlled in close proximity of the sample.

2. Development of the complex sawtooth

A sawtooth modulation will always lose steady state on its abrupt changing of the heating rate. Excluding all calorimeter effects, it could be shown, however, that as long as there are no instrument effects, Eq. (3)

should also hold when steady state is not reached, as long as one K applies to both calorimeters [6]. In an extensive study of calorimetry with sawtooth modulation it was found empirically that Eq. (3) with an adjustable τ could be used for analysis, not only of the data of the first harmonic $(v = 1)$, but also of the higher harmonics $(v = 3, 5, 7, \ldots)$ [7]:

$$C_p = \frac{A_{\mathrm{HF}}(v)}{A_{T_s}(v)v\omega} K(v\omega). \tag{4}$$

In analogy to Eq. (2), the dimensionless correction function $K(v\omega)$ in Eq. (4) may be written as

$$K(v\omega) = \sqrt{1 + \tau^2(v\omega)^2}, \tag{5}$$

where τ is now an empirical constant and may depend on instrument design, sample and reference properties (thermal conductivity, mass, and contact resistances), and at higher frequencies it may even lose its constancy with ω.

A simple, centrosymmetric sawtooth modulation about T_0 can be described by the Fourier series:

$$T(t) - T_0 = \frac{8A}{\pi^2}\left[\sin\omega t - \frac{1}{9}\sin 3\omega t + \frac{1}{25}\sin 5\omega t - \frac{1}{49}\sin 7\omega t + \frac{1}{81}\sin 9\omega t - \cdots\right], \tag{6}$$

where A is the modulation amplitude. Only the first harmonic in Eq. (6) has a big amplitude, the other amplitudes decrease quickly with frequency. Calculations of the heat capacities from the higher harmonics have, thus, less precision, still they can be used for heat capacity evaluation [8].

In order to improve the evaluation heat capacity from higher harmonic components, we first generated a complex sawtooth with identical harmonics for $v = 1, 3, 5$, and 7 as represented by [9]:

$$T_x(t) - T_0 = \frac{8A}{\pi^2}[\sin\omega t + \sin 3\omega t + 5\omega t + \sin 7\omega t - \frac{1}{9}\sin 9\omega t - \cdots]. \tag{7}$$

This complex sawtooth has 26 different segments and is represented in Fig. 1a. Next, we proposed a simplified complex sawtooth of 14 segments $T_x(t)$ with close to equal amplitudes for the four harmonics of the Fourier series of Eq. (6) which is much easier to generate. Its structure is shown in Fig. 1b and its Fourier series is given by [9]:

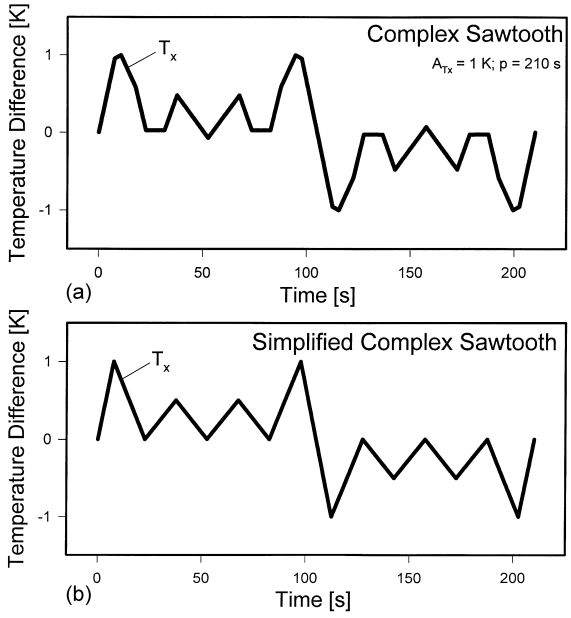

Fig. 1. Modulation with a complex sawtooth for a period p of 210 s. The upper figure (a) yields identical harmonics for $v = 1, 3, 5$ and 7. The lower figure (b) shows a simplified complex sawtooth as given in Eq. (8) with close to identical harmonics.

$$T_x(t) - T_0 = A[0.378\sin\omega t + 0.251\sin 3\omega t + 0.217\sin 5\omega t + 0.348\,7\omega t - \ldots]. \tag{8}$$

The programming steps of such a sawtooth are presented in Table 1 for an overall period of 420 s (30 s per sub-segment). This simplified complex sawtooth will be applied in this research and analyzed using Eqs. (4) and (5).

It will be shown that it is possible to produce this complex sawtooth with a standard DSC and to determine its various sinusoidal Fourier components to obtain simultaneous information on the sample response to modulation with different frequencies. The advantage of using the sawtooth modulation for the generation of a multiple frequency response of the sample is its ease of generation, even with a standard DSC. The disadvantage of the normally decreasing amplitudes of the harmonics with frequency is removed by choosing this special, complex sawtooth.

Table 1
Complex sawtooth program for $p = 420$ s

Segment No.[a]	Time (s)	Amplitude (K)	Heating rate (K min^{-1})
1	0–15	0.0–1.0	+4
2	15–45	1.0–0.0	−2
3	45–75	0.0–0.5	+1
4	75–105	0.5–0.0	−1
5	105–135	0.0–0.5	+1
6	135–165	0.5–0.0	−1
7	165–195	0.0–1.0	+2
8	195–225	1.0 to −1.0	−4
9	225–255	−1.0–0.0	+2
10	255–285	0.0 to −0.5	−1
11	285–315	−0.5–0.0	+1
12	315–345	0.0 to −0.5	−1
13	345–375	−0.5–0.0	+1
14	375–405	0.0 to −1.0	−2
15	405–420	−1.0–0.0	+4

[a] Note that in order to keep a centrosymmetric sawtooth, segments 1 and 15 are half segments.

The remaining problem of the loss of steady state is discussed. Results are obtained for sapphire and polystyrene samples. Similar data are derived for a power-compensated TMDSC and are described in [10] and the case of a standard DSC controlled closer to the heater is described in [11].

3. Experimental details

3.1. Instrumentation

For testing, the complex sawtooth modulation, a TA Instruments MDSC 2920^{TM} was used in the standard DSC mode of operation. The sample temperatures were calibrated using the onset temperatures of melting of indium (246.15 K) and water (273.15 K) at a heating rate of 10 K min^{-1}.

The heat-flow rate was approximately calibrated with the heat of fusion of indium and then corrected at the temperature of measurement with a heat capacity determination of sapphire. Dry nitrogen gas with a flow rate of 20 ml min^{-1} was purged through the DSC cell. Besides the calibration with sapphire, a baseline run with two empty aluminum pans under identical conditions was subtracted from each measurement. Experiments were made with 22.762 mg of sapphire and with two different sample masses of 7.629 and 22.142 mg of polystyrene (PS, MW = 280 000 Da). The sample pan weights were always about 23 mg and the reference pan weighed 21 mg.

Only the raw data as generated by the DSC were collected. All further calculations were performed with our own software, based on Mathematica 3.0^{TM}. As a consequence, similar results are expected from any DSC of similar control and precision.

3.2. Multifrequencies sawtooth modulation

Quasi-isothermally experiments were performed with the simplified, complex sawtooth modulation as presented by the program in Table 1 and shown in Fig. 1b. Fig. 2 illustrates the performance of the chosen calorimeter. The large, filled circles in Fig. 2a indicate the base temperature, T_0, and the programmed points of change in the rate of heating, as given in Table 1. Each sub-segment lasts 30 s and the harmonics with $v = 1, 3, 5, 7$ and 9 correspond to periods p of 420, 140, 84, and 60 and $46\frac{2}{3}$ s. The quasi-isothermally experiments were performed at 331.6 and 401.6 K for sapphire and polystyrene (PS). To check

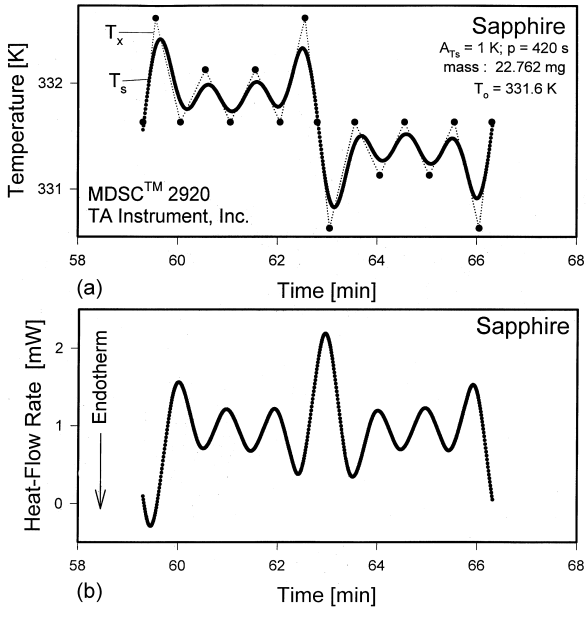

Fig. 2. An example of a run with a simplified, complex sawtooth of Eq. (8) and listed in Table 1 for a modulation period p of 420 s: (a) sample temperature $T_s(t)$; (b) heat-flow rate.

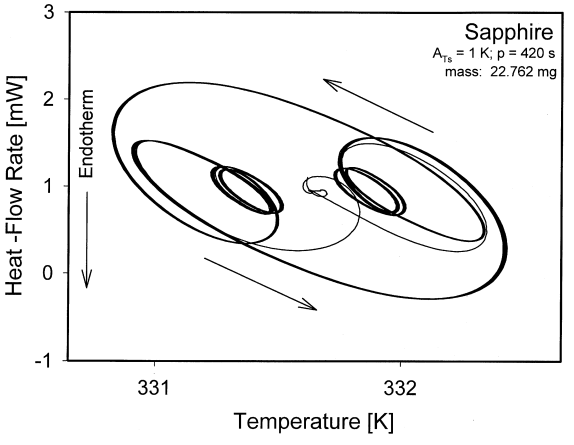

Fig. 3. Lissajous figure from the change of the heat-flow rate of Fig. 2b plotted against the change of the sample temperature of Fig. 2a.

on the reproducibility, 10 cycles of the modulation (or more) were repeated at each temperature. The Lissajous figures of one full 10-cycle run are shown in Fig. 3. The run starts and ends in the center. The first sub-cycle is only a half cycle and does not reach the later, far-right level reached after the combined segments $15 + 1$ in Table 1.

Also, the programmed level of T_0 is not reached in the second step in Table 1, as can also be seen in Fig. 2a. After the first two sub-cycles are completed, the further modulation is repeatable for the total experiment which ends after 10 repeats with the half-cycle 15. Measurement can, thus, be done when excluding the first two and the last half cycles. The quality of the repeatability can be judged from the width of the Lissajous figure in its various segments.

The calculation of the heat capacity, C_p, from the various harmonics in Eq. (8) requires the evaluation of the amplitudes of the heat-flow rate for each harmonic v, $A_{\mathrm{HF}}(v)$, and the corresponding sample temperature, $A_{T_s}(v)$ used in Eq. (4), and evaluation of $K(v\omega)$ by using Eq. (5). The time constant τ can be obtained by plotting the inverse of the squared, uncorrected heat capacity by setting $K(\theta\omega) = 1$ versus the square of the frequency [7,8]. The intercept of the plot at $(v\omega)^2 = 0$ is directly the inverse of the squared, τ-corrected heat capacity. The final step is the evaluation of the correction factor from the preliminary setting of the heat flow with the indium heat of fusion by comparison with a sapphire experiment. It should be noted that a baseline correction for asymmetry of the two calorimeters from a run with two empty pans, identical to the ones used in the measurement, is always required. For the evaluation the heat capacity with a complex sawtooth by TMDSC, one must make, thus, as in the standard DSC, three runs under the same conditions: an empty–empty run to establish the baseline, an empty–sapphire run to obtain the calibration factor for the temperature of measurement, and an empty–sample run to obtain the uncorrected heat capacity. Eqs. (4) and (5) indicate also that for very small frequencies (large modulation periods, p) the τ-correction becomes negligible.

4. Results

Figs. 2 and 3 show the typical raw data as obtained by the calorimeter. The data treatment, programmed in Mathematica 3.0™, is illustrated in Figs. 4 and 5. All of these figures refer to the calibration run with sapphire. The amplitudes resulting from the Fourier transform of the sample temperature, T_s, and the heat-flow rate, HF, are given in Table 2. They show that the complex sawtooth modulation produces similar amplitudes for sample temperatures and heat flow-rate amplitudes for the four harmonics ($v = 1, 3, 5,$ and 7). The ninth harmonic ($v = 9$), which was not adjusted to similar size by the complex sawtooth, has a much smaller amplitude and gives less precise data for the heat capacity. Finally, the second harmonic which should have no contribution for the centrosymmetric sawtooth modulation is, indeed, very small, indicating that despite the inability of the DSC to follow the rapid changes in programming of the temperature, the measurement remains centrosymmetric and the response is linear, as expected from a system which follows the Fourier equation of heat flow [1].

Figs. 4b and 5b illustrate that the experimental data of the sample temperature and heat-flow rate match closely the calculated sum of the first to the ninth harmonic for sapphire. This is not a requirement for measurement, but it means that by using the first five terms of the Fourier series, practically all of the experimental information has been made use of.

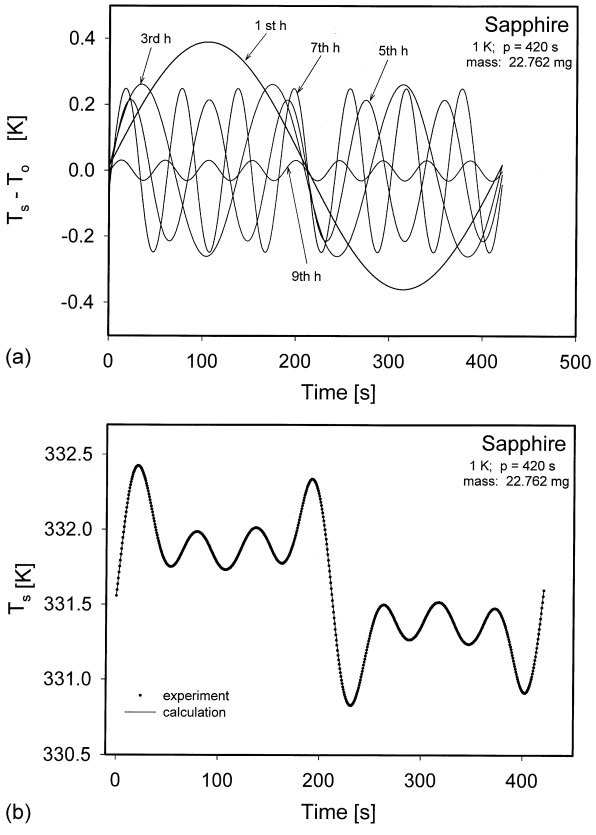

Fig. 4. Fourier analysis of the data for the sample temperature $T_s(t)$ in Fig. 2a: (a) harmonics $v = 1, 3, 5, 7$ and 9; (b) sum of the first to the ninth harmonics plotted together with the measured sample temperature.

Figs. 6–11 illustrate the final data treatment for three sets of sapphire and polystyrene measurements for two different masses and two temperatures. The parts (a) of the figures show the τ-uncorrected and corrected heat capacities as well as the influence of the calibration factor, and parts (b) of the figures display the evaluation the times τ according to Eq. (5). The changes in heat capacity were first calculated from Eq. (4) with $K(v\omega) = 1$ (after preliminary calibration with the heat of fusion of indium) as a function of modulation period, making use of the amplitudes of the first, third, fifth, seventh and ninth harmonic of the heat-flow rate and sample temperature (filled circles). This procedure is often proposed for the analysis of TMDSC data, but the results indicate that only for values of p above about 250 s is $K(v\omega)$ frequency independent when using a sawtooth modulation.

Figs. 6–11b illustrate the extrapolation of the uncorrected heat capacities, as suggested in Eq. (5) to evaluate τ. At zero frequency, the value of the corrected heat capacity can be read, and τ is given by the slope. Fig. 6b, yields at 331.6 K a τ of 6.94 s rad^{-1} for 22.8 mg of Al_2O_3. Using 7.6 mg of PS at the same temperature gives a τ of 5.4 s rad^{-1} (Fig. 7b), while for 22.1 mg PS, again at the same temperature, τ was 9.7 s (see Fig. 9b). At the increased temperature 401.3 K for 22.8 mg Al_2O_3, τ was estimated to be 6.06 s rad^{-1} (Fig. 10b) and for 22.1 mg PS, τ was 9.6 s rad^{-1} (see Fig. 11b). Clearly the equality $\tau = C_r/K$, suggested on the derivation of Eq. (3) does not hold for the sawtooth modulation. Using for PS the relaxation times τ and calibration factor K_{ave} calculated from the corrected heat capacities for Al_2O_3, the heat capacities of polystyrene marked by the open circles were established in Figs. 7a, 9a, and 11a. The internal precision for all five frequencies is about 1% for PS and 0.5% for PS, while the agreement with PS data from the ATHAS data

Table 2
Amplitudes of the various harmonics for sapphire at 331.6 K, $p = 420$ s, mass = 22.762 mg[a]

Number of the harmonics, v	Amplitude of T_s (K)	Amplitude of HF (mW)	Heat capacity[b] C_p (uc) (J K^{-1} mol^{-1})
1	0.3751	0.1176	81.91
(2)	(7.3×10^{-4})	(4.6×10^{-4})	–
3	0.2612	0.2388	78.43
5	0.21433	0.3117	73.34
7	0.2489	0.4759	66.935
(9)	(0.0308)	(0.0703)	(60.09)

[a] For the complex sawtooth in Fig. 1a and b.

[b] The heat capacity C_p (uc) is uncorrected for frequency and literature value of Al_2O_3, but corrected for the asymmetry of calorimeter and pan heat capacities.

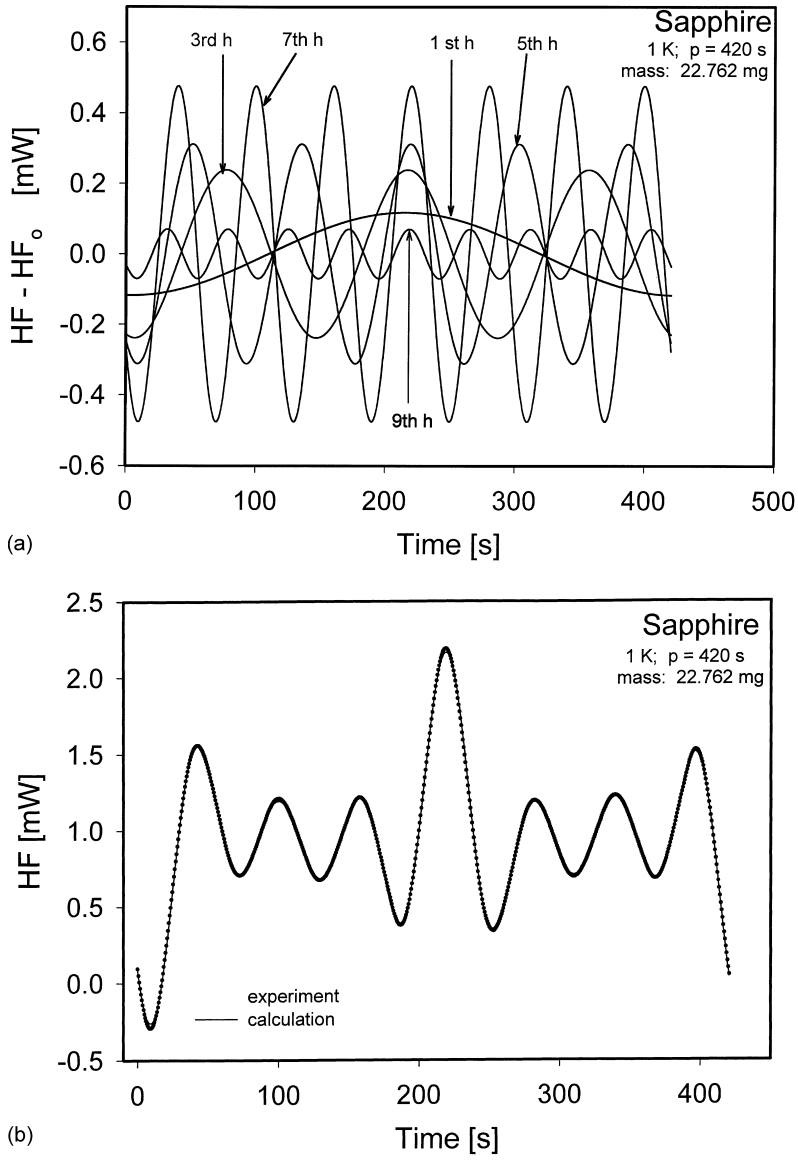

Fig. 5. Fourier analysis of the data of the heat-flow rate HF(t) in Fig. 2b: (a) harmonics $v = 1, 3, 5, 7$ and 9; (b) sum of the first to the ninth harmonics plotted together with the measured heat-flow rate.

bank [12] is within the 3–5% typical for data bank data on polymers.

5. Discussion

The results in Figs. 6–11 document that the proposed simplified sawtooth can be used for the measurement of frequency independent heat capacity with a precision that seems higher than for the standard DSC [1]. Once this is achieved, it should be possible to attempt to evaluate the frequency dependence of the heat capacity in transition regions, such as the glass transition region using the deviations from the functional relation for τ established in Figs. 6b–11b. The advantage of this somewhat difficult procedure is an

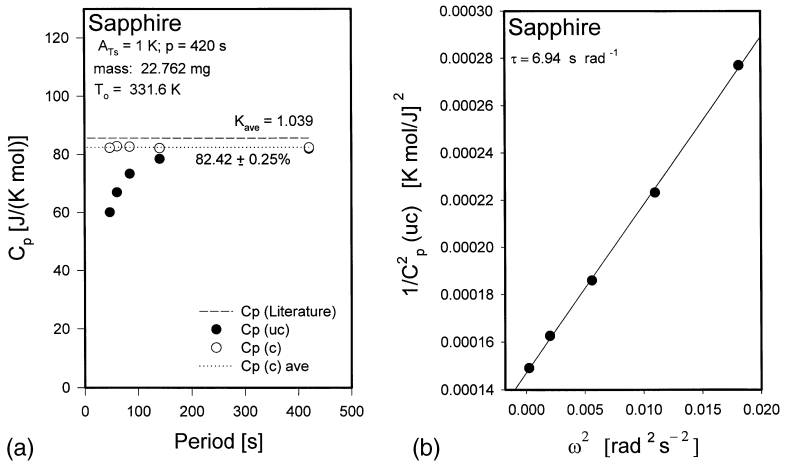

Fig. 6. Data and analysis for sapphire at 331.6 K: (a) plot of the uncorrected and corrected heat capacities; (b) plot of the uncorrected heat capacities to obtain τ from Eq. (5).

identical thermal history for all different frequencies which cannot be attained with separate experiments at different frequencies. We hope to carry out such experiments in the near future.

The dependence of τ in Eq. (5) on sample type, mass, and temperature can be derived from Figs. 6–11. As expected, smaller thermal conductivity leads to a larger τ (compare Figs. 8 and 9). A larger mass increases τ (compare Figs. 7 and 9). Higher temperature changes τ only little (compare Figs. 8 and 10 as well as Figs. 9 and 11). Although repeat experiments after longer time intervals changed τ only little, the correction factor K_{ave} may change as is also common in standard DSC (compare Figs. 6 and 7). The actual dependence on sample, mass and temperature has not been quantitatively determined since it is most likely necessary to calibrate each run with parallel empty–empty and empty–sapphire runs that must be completed before inadvertent changes upset the calibration factor K_{ave}.

The remaining question is the interpretation of τ. Its value between 5 and 10 s rad^{-1} affects the outcome of the experiments up to some 250 s. It must be remembered, however, that the period p plotted in Figs. 6–11

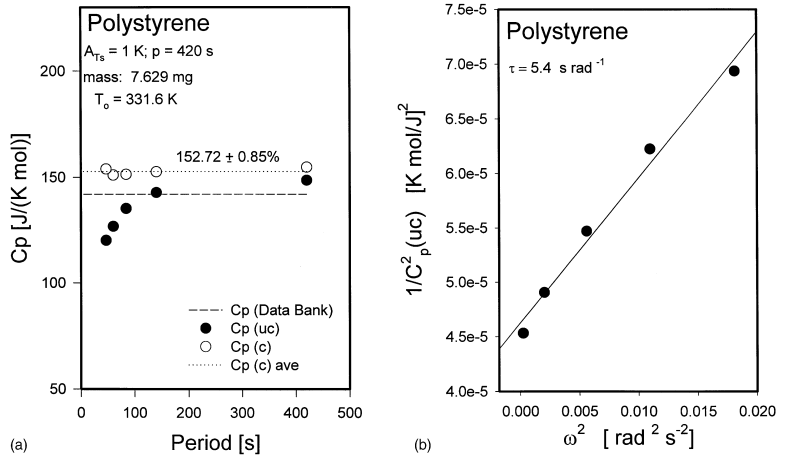

Fig. 7. Data and analysis for 7.63 mg of polystyrene at 331.6 K: (a) plot of the uncorrected heat capacities (●), as well as final data (○) using the τ-correction of Fig. 7b and the sapphire-calibration of Fig. 6; (b) plot of the uncorrected heat capacities to obtain τ from Eq. (5).

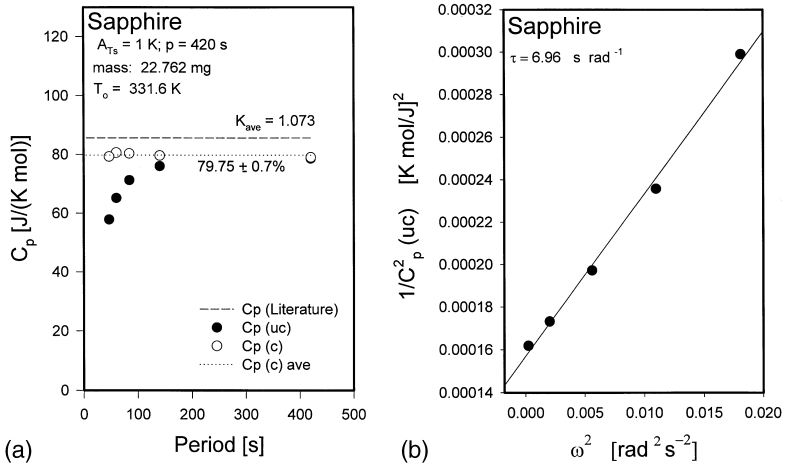

Fig. 8. Data and analysis for sapphire at 331.6 K: (a) plot of the uncorrected and corrected heat capacities; (b) plot of the uncorrected heat capacities to obtain τ from Eq. (5).

is made up of segments of 30 s each. Under the conditions of a negligible temperature gradient within the sample and strict adherence to the Fourier equation of heat flow, τ was shown to be strictly dependent on the heat capacity of the reference calorimeter only [6], which in the runs of Figs. 6–11 remained unchanged. We suggest that in the present calorimeter the Fourier equation of heat flow:

$$\frac{dT}{dt} = k\nabla^2 T, \tag{9}$$

where ∇^2 is the Laplacian operator $(\partial^2/\partial x^2 + \partial^2/\partial y^2 + \partial^2/\partial z^2)$, still holds, but that the condition of a negligible temperature gradient within the sample calorimeter is not reached within the sub-segments. As a result, the sequential segments of the complex sawtooth, reflected by the Lissajous figure in Fig. 3, refer to different internal temperature distributions. Relative to the first harmonic which represents an overall average over the total 420 s, the higher harmonics rely more on the response in the vicinity of the sharp changes in the heating rate, which occur every

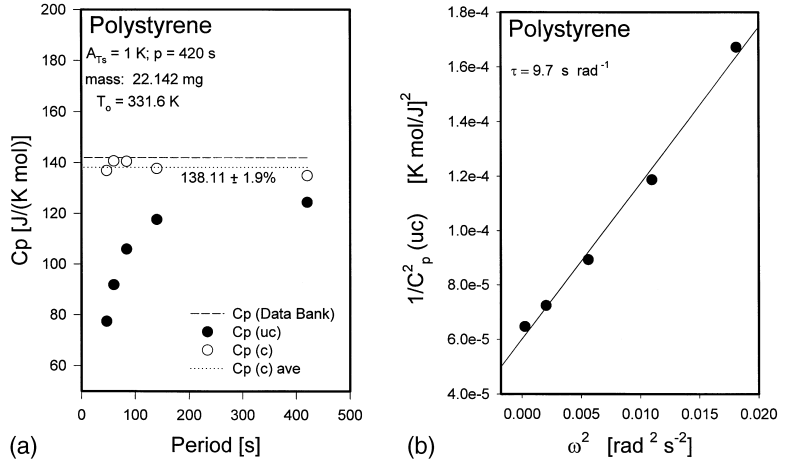

Fig. 9. Data and analysis for 22.1 mg of polystyrene at 331.6 K: (a) plot of the uncorrected heat capacities (●), as well as final data (○) using the τ-correction of Fig. 9b and the sapphire-calibration of Fig. 8; (b) plot of the uncorrected heat capacities to obtain τ from Eq. (5).

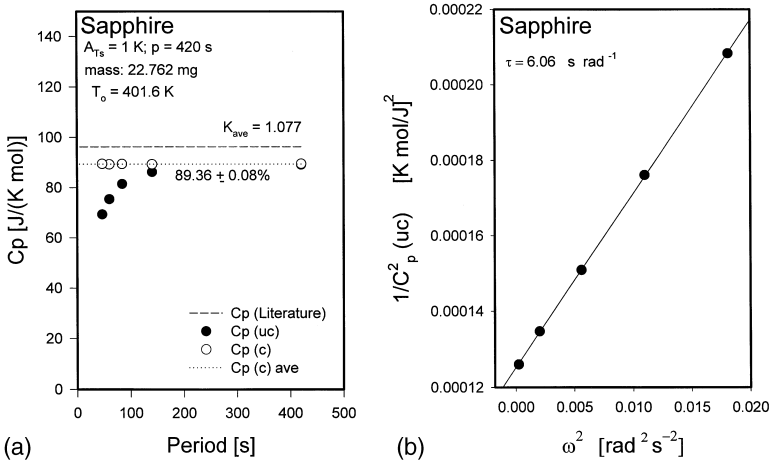

Fig. 10. Data and analysis for sapphire at 401.6 K: (a) plot of the uncorrected and corrected heat capacities; (b) plot of the uncorrected heat capacities to obtain τ from Eq. (5).

30 s (see Fig. 5b). During the change of the heating rate, however, the apparent heat capacity is reduced since the new steady state is approached only gradually.

A final remark concerns the common practice of baseline subtraction for the correction of asymmetry in the calorimeter. Despite the fact that Eq. (9) is a linear differential equation for which sums of different solutions are again solutions of Eq. (9), the Fourier series of Eq. (6) requires strict additivity of components of the response to be analyzed [9]. The heat-flow rates of the baseline run with empty sample and reference pans, however, can only be subtracted from the sample and reference runs in the regions of steady state (horizontal segments in the heat-flow rate). Mathematically this method of baseline subtraction is, thus, not sound, although the result is to be preferred over the case of no correction at all. Experimentally it would be preferable to use no empty reference pan and select a DSC head with high symmetry, so that the correction is negligible. Another method of correction in is the frequency domain, where, however the phases of the to-be-subtracted heat capacities must be known [13].

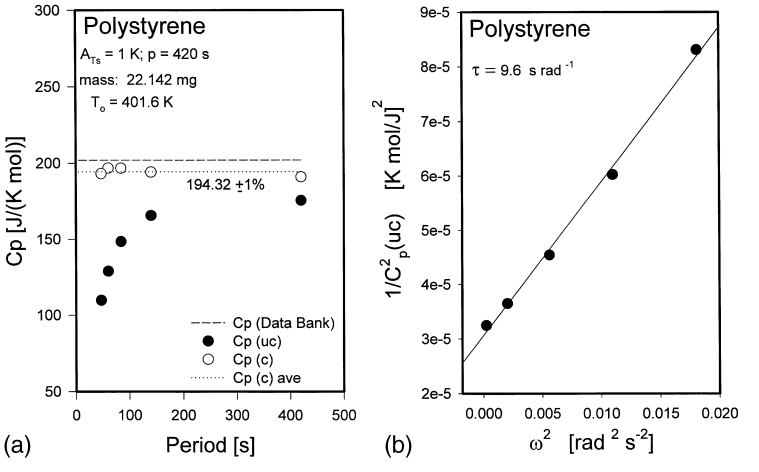

Fig. 11. Data and analysis for 22.1 mg of polystyrene at 401.6 K: (a) plot of the uncorrected heat capacities (●), as well as final data (○) using the τ-correction of Fig. 11b and the sapphire-calibration of Fig. 10; (b) plot of the uncorrected heat capacities to obtain τ from Eq. (5).

6. Conclusions

In this paper it is shown that using sawtooth modulation the evaluation of heat capacity from a single experiment is possible. One must extrapolate the heat capacity from the amplitudes of the first and higher harmonics of the Fourier transforms of the sample temperature and heat-flow rate or use modulation times that exceed 200 s. After these corrections are done, sub-segments of 30 s can be included in the evaluation of the response to a complex sawtooth. Eqs. (4) and (5) allow the on-line evaluation from a single, complex sawtooth that never reaches steady state. It is suggested that the time-dependence of the calorimeter response is due to a changing temperature gradient within the sample. The time constant for this correction is 5–10 s rad^{-1}. Parallel papers on a power-compensated DSC [10] and a heat-flux calorimeter, controlled close to the heater [11], are shown to behave somewhat differently, i.e., before making use of sawtooth modulation, an extensive investigation of the calorimeter to be used must be undertaken.

The advantages of using the proposed complex sawtooth modulation in the determination of the heat capacity are as follows: (a) a single experiment eliminate the apparent frequency dependence of the heat capacity: (b) better precision of the determination of C_p is expected than from higher harmonics of a simple sawtooth modulation as carried out before [10]; (c) the same experimental conditions exist for all frequencies tested because of the exact correspondence of the sample geometry and history which is of particular importance for samples that have an inherent frequency dependence of the heat capacity, as is observed in the glass transition region; (d) the extrapolation suggested in Eq. (5) can be included in the data analysis software for ease of operation; (e) the experience gained from the present investigation can advance the construction of better DSC equipment.

Acknowledgements

This work was financially supported by the Division of Materials Research, NSF, Polymers Program, Grant No. DMR-9703692 and the Division of Materials Science, Office of Basic Energy Sciences, DOE at Oak Ridge National Laboratory, managed by Lockheed Martin Energy Research Corporation for DOE, under contract No. DE-AC05-96OR22464.

References

[1] B. Wunderlich, Thermal Analysis, Academic Press, New York, 1990. For an update, see our computer-assisted lecture course of 36 lectures on about 3000 screens, published on the World Wide Web (URL: http://web.utk.edu/~athas/courses/tham99.html), 1999.
[2] P.S. Gill, S.R. Sauerbrunn, M. Reading, J. Therm. Anal. 40 (1993) 931.
[3] M. Reading, A. Luget, R. Wilson, Thermochim. Acta 138 (1994) 295.
[4] A. Boller, Y. Jin, B. Wunderlich, J. Therm. Anal. 42 (1994) 307.
[5] B. Wunderlich, Y. Jin, A. Boller, Thermochim. Acta 238 (1994) 277.
[6] B. Wunderlich, A. Boller, I. Okazaki, K. Ishikiriyama, W. Chen, M. Pyda, J. Pak, I. Moon, R. Androsch, Thermochim. Acta 330 (1999) 21.
[7] R. Androsch, I. Moon, S. Kreitmeier, B. Wunderlich, Thermochim. Acta 357/358 (2000) 267.
[8] R. Androsch, B. Wunderlich, Thermochim. Acta 333 (1999) 27.
[9] B. Wunderlich, R. Androsch, M. Pyda, Y.K. Kwon, Thermochim. Acta 348 (2000) 267.
[10] Y.K. Kwon, R. Androsch, M. Pyda, B. Wunderlich, Thermochim. Acta 367/368 (2001) 203.
[11] J. Pak, B. Wunderlich, Thermochim. Acta, this issue.
[12] U. Gaur, B. Wunderlich, J. Phys. Chem., Ref. Data, 11 (1982) 313; see also the ATHAS data bank on the Internet (URL: http://web.utk.edu/~athas).
[13] K. Ishikiriyama, B. Wunderlich, J. Therm. Anal. Calorimetry 50 (1997) 337.